Available online at www.sciencedirect.com
SCIENCE DIRECT®
ELSEVIER
Physica D 183 (2003) 245–259
PHYSICA D
www.elsevier.com/locate/physd

Analytic solutions of a nonlinear convective equation in population dynamics

L. Giuggioli*, V.M. Kenkre

Consortium of the Americas for Interdisciplinary Science and Department of Physics and Astronomy, University of New Mexico, Albuquerque, NM 87131, USA

Received 3 February 2003; received in revised form 28 March 2003; accepted 23 May 2003
Communicated by R. Roy

Abstract

Analytic solutions are presented for a simple nonlinear convective equation of use in population dynamics. In spite of its simplicity the equation predicts rich behavior including a velocity inversion transition. Stability considerations are also presented.

PACS: 87.17.Aa; 87.17.Ee; 87.17.Jj

Keywords: Transport in biological systems; Convection; Logistic Nonlinearity; Fisher equation

1. Introduction

Population dynamics of bacterial colonies have often been analyzed [1–5] with the help of the Fisher equation [6] which combines diffusion with a logistic nonlinearity [7–10]. Identical or related equations have also appeared in the study of the dynamics of infected mice in hantavirus epidemics [11–13]. Exact solutions of the Fisher equation are not known except in very special conditions [7]. Analytic research regarding entities that are similar to the Fisher equation [14–16] has, therefore, the potential to be of use in diverse situations in population dynamics. The purpose of the present paper is to report on analytic solutions we have found of an equation which is similar to, but simpler than, the Fisher equation, and which might be applicable to systems such as bacterial colonies in certain situations.

Because of its potential for the understanding of propagation of infection in living tissue, a lot of interest has been generated theoretically as well as experimentally in the study of bacteria in Petri dishes. Experiments have been carried out [3,4] to verify an interesting extinction transition predicted by a theoretical analysis [5]. That analysis has focused on a form of the Fisher equation which includes a 'wind' term responsible for convection in addition to diffusion, and wherein the rate of growth of the bacteria is spatially dependent. The significance of such a wind term is that it describes the effect of a moving mask which is part of the experiments. The method of analysis [5]

* Corresponding author. Tel.: +1-505-2770848; fax: +1-505-2771520.
E-mail addresses: giuggiol@unm.edu (L. Giuggioli), kenkre@unm.edu (V.M. Kenkre).

0167-2789/$ – see front matter © 2003 Elsevier B.V. All rights reserved.
doi:10.1016/S0167-2789(03)00176-3

has employed techniques based on linearization of the logistic nonlinearity. Our interest is in systems wherein the nonlinearity is central but diffusion is negligible, or at least quantitatively less important than the convection term. Therefore, starting with the general equation

$$\frac{\partial u(x,t)}{\partial t} + v(t)\frac{\partial u(x,t)}{\partial x} = a(x,t)u(x,t) - b(x,t)u(x,t)^2 + D\frac{\partial^2 u(x,t)}{\partial x^2}, \tag{1}$$

where $u(x,t)$ represents the population density (e.g., of a bacteria colony) at position x at time t, which grows at a rate $a(x,t)$ and is limited by a mutual competition–annihilation coefficient $b(x,t)$, is subjected to convection at velocity $v(t)$, and moves diffusively with coefficient D, we consider the case wherein D may be neglected

$$\frac{\partial u(x,t)}{\partial t} + v(t)\frac{\partial u(x,t)}{\partial x} = a(x,t)u(x,t) - b(x,t)u(x,t)^2, \tag{2}$$

obtain exact analytic solutions, and show that interesting conclusions can be extracted from the solutions.

The paper is organized as follows. In Section 2 we analyze the case of constant a, b, and v. We observe unexpected phenomena such as a transition in the propagation direction depending on the steepness of the initial density and a curious reversal in the direction of propagation for certain initial conditions. Time-dependent v and a are studied in Sections 3.1 and 3.2, respectively. The case of spatially dependent a is the subject of Section 3.3. Stability considerations are given in Section 4, and conclusions in Section 5.

2. Constant coefficients

When a, b and v are constants, Eq. (2) becomes

$$\frac{\partial u(x,t)}{\partial t} + v\frac{\partial u(x,t)}{\partial x} = au(x,t) - bu(x,t)^2. \tag{3}$$

The simple transformation $\phi(x,t) = 1/u(x,t)$ converts Eq. (3) to

$$\frac{\partial \phi(x,t)}{\partial t} + v\frac{\partial \phi(x,t)}{\partial x} + a\phi(x,t) = b, \tag{4}$$

which is solved at once to yield

$$u(x,t) = \frac{u_0(x-vt)}{\mathrm{e}^{-at} + (b/a)(1-\mathrm{e}^{-at})u_0(x-vt)}, \tag{5}$$

where $u_0(x)$ is $u(x,0)$, i.e., the initial shape of the density. Eq. (5) is an exact solution valid for arbitrary initial conditions. It shows that the initial shape $u_0(x)$ travels at first with the medium velocity v while, at long times, the behavior depends on the long-time limit of $\exp(-at)u_0^{-1}(x-vt)$. If the spatial dependence of $u_0(x)$ is such that this limit is zero, u tends to a/b. Otherwise, the solution becomes a traveling wave at long times.

2.1. Traveling fronts

Traveling fronts (traveling waves with constant velocity and shape) can be shown to obey Eq. (3). Inserting the ansatz $u(x,t) = u_{\mathrm{front}}(x-ct)$ in Eq. (3), such a solution can be written as

$$u_{\mathrm{front}}(x-ct) = \frac{a}{b}\frac{1}{1+\mathrm{e}^{-(a/(v-c))(x-ct)}}, \tag{6}$$

where the constant of integration has been chosen so that the front at $t=0$ is centered around $x=0$. We see that the parameter c characterizes both the propagation velocity and the steepness. If the shape is a fall from a/b at

$x = -\infty$ to 0 at $x = +\infty$, c is larger than v. If the shape is a rise from 0 at $x = -\infty$ to a/b at $x = +\infty$, c is smaller than v. We will call these two kinds of fronts 'right' front and 'left' front, respectively. For right fronts higher c's correspond to shallower profiles. The opposite is true in the latter case.[1]

If the initial distribution is given by a right front, the corresponding solution ($c > v$) propagates to the right. If the initial distribution is given by a left front profile exactly equal to $g(x) = (a/b)[1 + \exp(-ax/v)]^{-1}$, the corresponding solution ($c = 0$) is stationary. For an initial profile steeper than $g(x)$, $0 < c < v$, i.e., the (left) front propagates to the right. For an initial profile shallower than $g(x)$, $c < 0$, i.e., the (left) front propagates to the left. In other words, a right front propagates always in the direction of the medium velocity. A left front is not so restricted: its shape determines in which direction it moves or whether it moves at all.

2.2. Initial exponential tails

When the initial shape does not coincide with one of the traveling fronts, but involves exponential tails, there is a transient during which the shape changes to that of an appropriate traveling front solution, followed by propagation at the front velocity as described in Section 2.1. An initial right leading edge always evolves into a right moving front. If $u_0(x)$ as $x \to -\infty$ is steeper (shallower) than $\exp(ax/v)$, a left front will eventually propagate to the right (left). The terms 'left' and 'right' front have the meaning explained in Section 2.1.

The value c of the eventual velocity attained by the distribution can be determined with great accuracy from the (exponential) spatial dependence of $u_0(x)$ at infinity. Through an analysis similar to one used in the past for the study of front propagation in the Fisher equation [17], we consider only the leading edge $\bar{u}(x, t)$ of $u(x, t)$ in Eq. (3). Neglecting $\bar{u}^2$, and looking for a propagating solution of the form $\bar{u}(x - ct)$, we obtain

$$c = v - a\frac{\bar{u}}{\bar{u}'}, \tag{7}$$

which relates the eventual velocity c to the growth rate a, and the behavior of $u_0(x)$ at $x \to \pm\infty$. Here, $\bar{u}'$ is the spatial derivative of $\bar{u}$. If $\bar{u}(x) \propto \exp(\pm x/\sigma)$ where the $+$ $(-)$ sign represents a left (right) leading edge, Eq. (7) gives the simple recipe $c = v \mp a\sigma$. The $-$ $(+)$ sign is for the left (right) leading edge. Numerical calculations fully verify this recipe. Eq. (7) also shows that for initial pulses with exponential tails, the left face has a value of the propagating velocity c always smaller than the right face. This in turn implies a broadening of the initial pulse as time evolves.

In Fig. 1, we show an example of the evolution of an initial pulse with exponential tails. We have chosen the values of v, a, and σ such that $c = 0$ for the left face according to Eq. (7). The initial condition is set to be $u_0(x) = [\mathrm{sech}(x/\sigma)]^{\alpha}$, whose corresponding $\bar{u}(x) \propto \exp(\alpha x/\sigma)$ for the left face. With a velocity $v = a\sigma/\alpha$, the propagation velocity becomes exactly zero. After an initial transient in which $u_0(x)$ moves to the right, the left face evolves into the front solution of Eq. (6) with velocity $c = 0$, while the right face evolves into the front solution with velocity $c = 2v$.

Initial pulses with exponential tails exhibit, thus, a transition in the direction of propagation depending on the steepness of their left face. Does such a transition occur if the left face is *qualitatively* (not merely quantitatively) different than an exponential? We pursue this question in the next subsection.

2.3. Initial non-exponential tails

Non-exponential initial tails mean that $\bar{u}/\bar{u}'$ is either exactly zero or it is not constant. For the non-constant case, Eq. (7) suggests that the propagation velocity is variable. This has been verified both numerically and through a

[1] Throughout the paper we assume, unless it is mentioned otherwise, that $v > 0$, i.e., we suppose that the convection term is to the right. All the results can be trivially reformulated for the case $v < 0$.

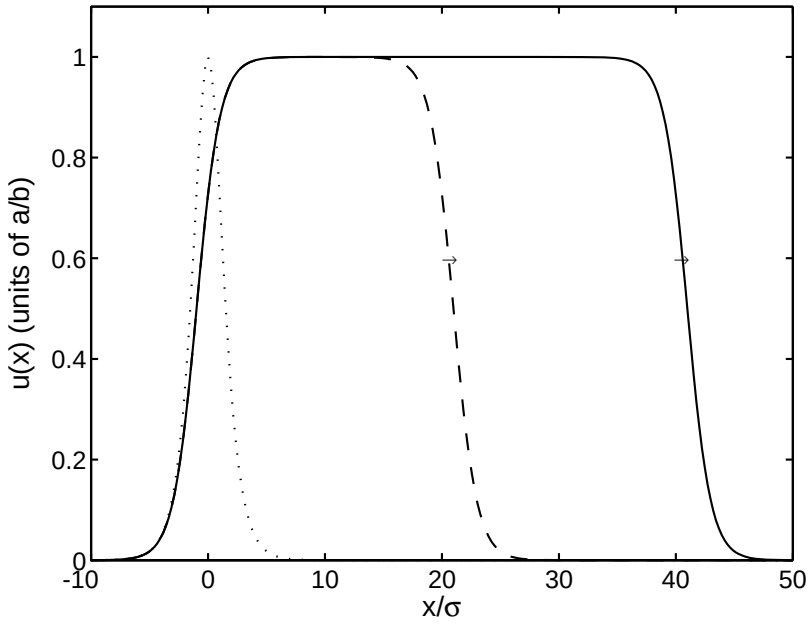

Fig. 1. Example of an evolution of $u(x,t)$ with initial exponential tails when the left front stays steady: $u_0(x) = [\mathrm{sech}(x/\sigma)]^{\sqrt{2}}$ with $v/(a\sigma) = 1/\sqrt{2}$. The distribution initially moves to the right but later adjusts its left profile to the traveling front profile with velocity $c = 0$, while the right profile evolves as a front with velocity $c = 2v$. The dotted, dashed and solid lines correspond, respectively, to $t = 0$, 10, 20 in units of $1/a$.

stability analysis of the front solutions (see Section 4). The movement of a right leading edge is always to the right. If initially the right face is shallower (steeper) than an exponential, the velocity increases (decreases) and the steepness decreases (increases).

For a left leading edge, similarly to Section 2.2, the motion can be opposite to the direction of the medium velocity. A profile shallower than an exponential will eventually move to the left, decreasing its steepness and increasing its velocity. If the left profile is steeper than an exponential, the movement will eventually be to the right with an increasing steepness and a decreasing velocity. In Fig. 2 we have plotted a situation in which the two faces move in opposite directions, i.e., when the left and right faces are shallower than an exponential. It is evident from the plot that there is an increase in the velocity of each face.

The growth of the velocity for shallow initial tails is unbounded while the decrease of the velocity for steep initial tails is bounded. If the steepness of a leading edge becomes infinite, the ratio $\bar{u}/\bar{u}'$ goes to zero and Eq. (7) dictates that the velocity is now constant and exactly equal to the medium velocity v. Clearly, what has just been described is a limiting situation for $t \to +\infty$. However, if initially $u_0(x)$ is such that $\bar{u}(x) \propto \Theta(x - x_1)$ for its left face, $\bar{u}/\bar{u}' = 0$ for $x < x_1$ and its velocity is exactly v. If a similar condition applies for the right face, it translates to a constant propagation for the whole profile at the medium velocity v. We observe that, for initial conditions with compact support, i.e., when $u_0(x)$ vanishes outside a finite interval, there is a transient during which the initial shape rearranges itself into a square pulse with height a/b and width equal to its initial value, while simultaneously moving to the right. From then on, the square pulse proceeds without changing shape. Fig. 3 shows an example of such a scenario.

A simple way to verify if an initial pulse indeed develops into a front solution is to plot the area $A(t)$

$$A(t) = \int_{-\infty}^{+\infty} \mathrm{d}\left(\frac{x}{\sigma}\right) u(x,t), \tag{8}$$

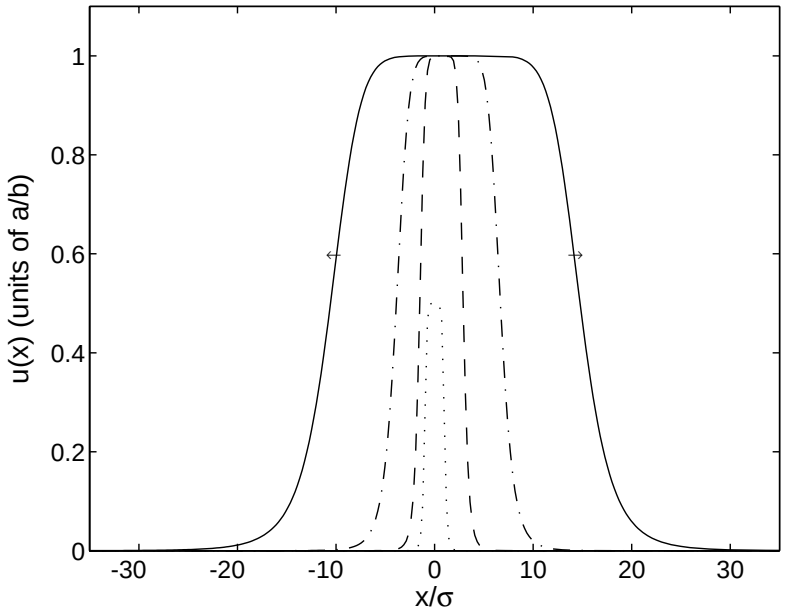

Fig. 2. Evolution in time for an initial pulse with non-exponential tails. At time $t = 0$, $u_0(x) = [1 + (x/\sigma)^8]^{-1}/2$ with $v/(a\sigma) = 0.1$. Even with a convection (medium velocity) to the right, the left face moves to the left, i.e., in the *opposite* direction. The dotted, dashed, dash-dotted, and solid lines corresponds, respectively, to $t = 0$, 7, 14, 21 in units of a/b.

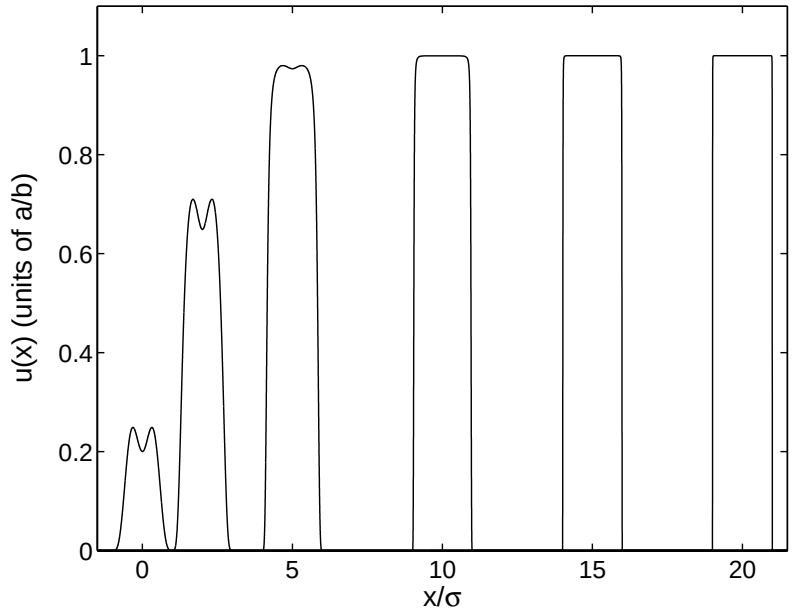

Fig. 3. Example of evolution for an initial condition with compact support with $v/(a\sigma) = 1$ and $u_0(x) = [\Theta(x/\sigma + 1) - \Theta(x/\sigma - 1)]$ $[0.2 + 2(x/\sigma)]^2[1 - (x/\sigma)^2]^{9/2}$, where the first square bracket gives the cut-off, the second the dip in the middle, and the third the basic profile. From left to right, the curves are at $t = 0$, 2, 5, 10, 15, and 20, respectively, in units of $1/a$. After the steady profile (step function) is reached (around at $= 20$), the evolution is that of a solitary wave.

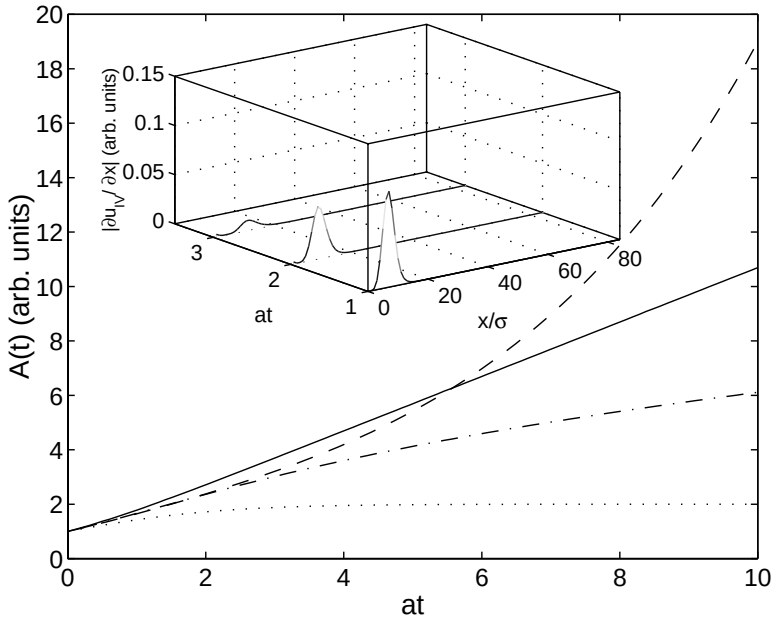

Fig. 4. Evolution in time of the area $A(t)$ for four different initial conditions. $u_{\mathrm{I}}(x,0) = 2[\Theta(x/\sigma+1)-\Theta(x/\sigma-1)][1-(x/\sigma)^2]^{1/2}/\pi$ for the dotted line, $u_{\mathrm{II}}(x,0) = \exp[-(x/\sigma)^2]/\sqrt{\pi}$ for the dash-dotted line, $u_{\mathrm{III}}(x,0) = [\mathrm{sech}(x/\sigma)]^2/2$ for the solid line, and $u_{\mathrm{IV}}(x,0) = 2\sin(\pi/4)[1+(x/\sigma)^4]^{-1}/\pi$ for the dashed line. u_{I} and u_{III} are the only cases in which, after an initial transient, a traveling front solution develops. For u_{II} and u_{IV}, instead, velocity and shape of the leading edges is changing in time, thus making the area increase nonlinearly. The four curves have been chosen normalized so that $A_i(0) = 1$ with $v/(a\sigma) = 1$. The inset shows the variation of the steepness of the right leading edge of u_{IV} at time $t = 1$, 2, and 3, respectively, in units of $1/a$.

where σ is the characteristic width of the initial shape. If the leading edges of u evolve to front solutions, $A(t)$ increases linearly in time at a rate proportional to the difference in the velocities of the right and left fronts. If $A(t)$ does not show a linear dependence, it means that at least one of the two faces has not settled into a propagating front: it is in the process of changing its shape and velocity. Fig. 4 displays the area $A(t)$ as a function of time for four qualitatively different initial shapes: u_{I}, u_{II}, u_{III}, and u_{IV}. All shapes have been taken symmetric for simplicity. The dotted line corresponds to an initial condition with compact support (I), the dash-dotted line to one with steep tails (II), the solid line to one with exponential tails (III), and the dashed line to one with shallow tails (IV). In case I, $A(t)$ flattens out since both leading edges move with velocity $c = v$ without changing shape. In case III, both faces settle into front solutions moving at constant velocity and without changing shape: $A(t)$ increases linearly. In cases II and IV, however, the velocity and shape of the leading edges are changing in time. In the former case the velocity is decreasing and the steepness is increasing. The reverse is true for the latter case. The increase of $A_{\mathrm{II}}(t)$ is shallower than $A_{\mathrm{IV}}(t)$, the former being sublinear and the latter superlinear. If $u(x,t)$ is integrable over all space, the time dependence of $A(t)$ can be determined analytically. We give two examples below:

- If $u_0(x) = [1+(|x|/\sigma)^\alpha]^{-1}/N$, with $\alpha > 0$ and the normalization constant $N = 2\pi/[\alpha\sin(\pi/\alpha)]$, we have

$$A(t) = \mathrm{e}^{at}\left[1+\frac{b}{Na}(\mathrm{e}^{at}-1)\right]^{(1-\alpha)/\alpha}. \tag{9}$$

  Because the rate of increase of the area is proportional to the difference in the velocity between the right and left faces, v does not appear in (9). The superlinear increase is actually exponential at long times, $A(t) \sim \exp(at/\alpha)$ but linear at short times, $A(t) \sim 1+[(1-\alpha)b/(\alpha N)]t$. Since $1/N$ equals $u_0(0)$ (the maximum of $u_0(x)$), for

values of N sufficiently smaller than b/a, $A(t)$ shows a minimum which represents the transient during which $u(x,t)$ decreases its peak value to the saturation value a/b.

- If $u_0(x) = \mathrm{sech}(x/\sigma)/\pi$, an integration over all space gives

$$A(t) = \begin{cases} \dfrac{4}{\pi\sqrt{\mathrm{e}^{-2at} - \alpha^2(t)}} \tan^{-1}\left(\dfrac{\sqrt{\mathrm{e}^{-2at} - \alpha^2(t)}}{\mathrm{e}^{-at} + \alpha(t)}\right) & t < \dfrac{\ln(1 + (\pi a/b))}{a}, \\ \dfrac{2}{\pi\sqrt{\alpha^2(t) - \mathrm{e}^{-2at}}} \ln\left(\dfrac{\alpha(t) + \mathrm{e}^{-at} + \sqrt{\alpha^2(t) - \mathrm{e}^{-2at}}}{\alpha(t) + \mathrm{e}^{-at} - \sqrt{\alpha^2(t) - \mathrm{e}^{-2at}}}\right) & t \geq \dfrac{\ln(1 + (\pi a/b))}{a}, \end{cases} \tag{10}$$

where $\alpha(t) = [1 - \exp(-at)]b/(\pi a)$. The expected linear time dependence can be recovered in the two limits: for $t \to +\infty$ $A(t) \sim 2\ \ln(2)a^2 t/b$ and for $t \to 0$ $A(t) \sim 1 + 2bt[a\pi^2/(2b) - 1]/\pi^2$. As in the first example, for the same reason at initial times $A(t)$ can have a minimum if $a/b < 2/\pi^2$.

2.4. Phenomenon of velocity inversion

We have seen that, except for initial conditions with compact support, non-exponential tails do not lead to traveling fronts. A remarkable phenomenon that can occur for such non-exponential initial shapes is an inversion in the propagation direction of the *left* face. If the initial profile (of the left face) is shallow (steep) enough, the propagation can be first to the right (left) and later to the left (right). Fig. 5 shows this curious behavior for $u_0(x) = \exp[-(x/\sigma)^2]/2$, i.e., for the case of a steep $\bar{u}(x)$.

The velocity inversion can be interpreted as follows. In Eq. (3) the propagation arrow is determined by the combined effect of two terms: $-vu_x$ and au. For a left face $-vu_x$ accounts for a reduction of u while au gives an increase of u. If $-vu_x$ prevails, the movement is to the right, otherwise it is to the left. Thus, even in the case of a shallow initial tail, the term $-vu_x$ can be made bigger than au with a big enough velocity v. The movement in that

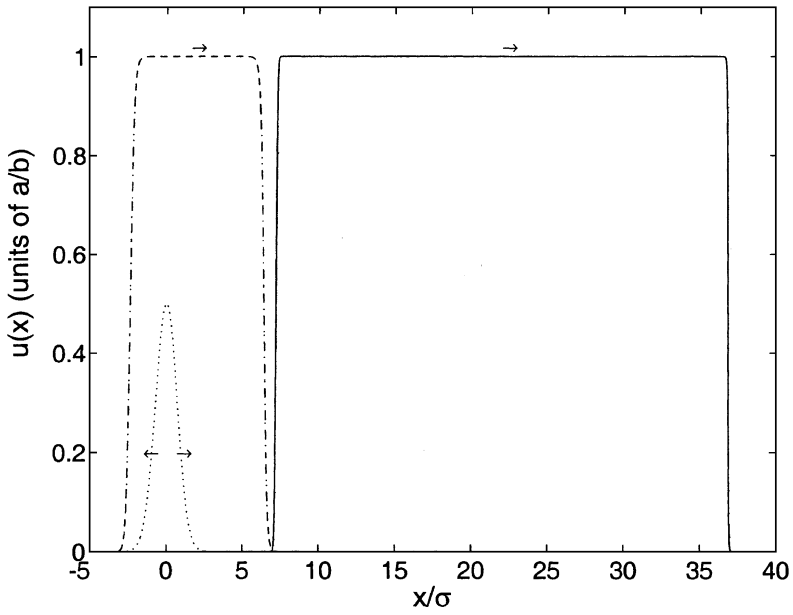

Fig. 5. Velocity inversion of the left front. The initial shape (dotted line) is a Gaussian. The dash-dotted and solid lines are at time $t = 20$ and 220 in units of $1/a$. Around time at $= 22$, the left front changes its direction of propagation and proceeds then to move to the right, i.e., in the direction of v. Parameters are chosen such that $v/(a\sigma) = 0.1$.

case is initially to the right. However, since the profile is becoming shallower as time evolves, at a certain moment $-vu_x$ becomes smaller than au and the propagation direction is reversed. A similar behavior happens for steep initial tails but now the initial movement is to the left if the velocity v is small enough. This transition happens only for the left face. For the right face the two terms do not compete. They both contribute to a right movement. In other words we can say that the value of the right-hand side of Eq. (7) decreases or increases up to the point when $c = 0$. At that moment an inversion in the direction of propagation appears.

3. Variable coefficients

Consider, first, the situation wherein the velocity v and the growth term a are time-dependent but the only position dependence is in the competition term b. Thus,

$$\frac{\partial u(x,t)}{\partial t} + v(t)\frac{\partial u(x,t)}{\partial x} = a(t)u(x,t) - b(x,t)u(x,t)^2. \tag{11}$$

The corresponding transformed equation for $\phi = 1/u$,

$$\frac{\partial \phi(x,t)}{\partial t} + v(t)\frac{\partial \phi(x,t)}{\partial x} + a(t)\phi(x,t) = b(x,t) \tag{12}$$

is solved at once to yield

$$\phi(x,t) = \mathrm{e}^{-\int_0^t \mathrm{d}s\, a(s)}\phi_0\left(x - \int_0^t \mathrm{d}s\, v(s)\right) + \int_0^t \mathrm{d}t'\, \mathrm{e}^{-\int_{t'}^t \mathrm{d}s\, a(s)} b\left(x - \int_{t'}^t \mathrm{d}s\, v(s), t'\right) \tag{13}$$

and, therefore, $u(x,t)$ explicitly. We examine two particular cases in Sections 3.1 and 3.2, and return to spatially dependent growth rates in Section 3.3.

3.1. Time-dependent medium velocity

Let the medium velocity be oscillatory and given by

$$v(t) = v\cos(\omega t). \tag{14}$$

Taking a and b to be independent of time and space, we obtain

$$u(x,t) = \frac{1}{(\mathrm{e}^{-at}/u_0[x - (v/\omega)\sin\omega t]) + (b/a)(1 - \mathrm{e}^{-at})}, \tag{15}$$

which shows that the distribution oscillates around the origin while increasing its total area as in the case of constant velocity. Unlike the constant velocity case, the profile and the velocity are continuously changing in time. As for the case of constant coefficients, the steepness of $u_0(x)$ determines the direction and the velocity at which the leading edges are propagating. For an initial (symmetric) shape with tails shallower than $\exp(|x|a/v)$, the leading edges of u always move outwards independently of the medium velocity direction. For an initial (symmetric) shape with tails steeper than $\exp(|x|a/v)$, the leading edges change propagation direction as the medium velocity changes direction. To describe this behavior, we consider the normalized mean-squared-displacement $\langle x^2\rangle$, which, for symmetric initial pulse of characteristic width σ, obeys

$$\langle x^2\rangle = \left(\frac{v}{\omega\sigma}\right)^2 \sin^2(\omega t) + \frac{\int_{-\infty}^{+\infty} \mathrm{d}(y/\sigma)(y/\sigma)^2 p(y,t)}{\int_{-\infty}^{+\infty} \mathrm{d}(y/\sigma)p(y,t)}, \quad p(y,t) = \frac{1}{\exp(-at)u_0^{-1}(y) + [1 - \exp(-at)]b/a}. \tag{16}$$

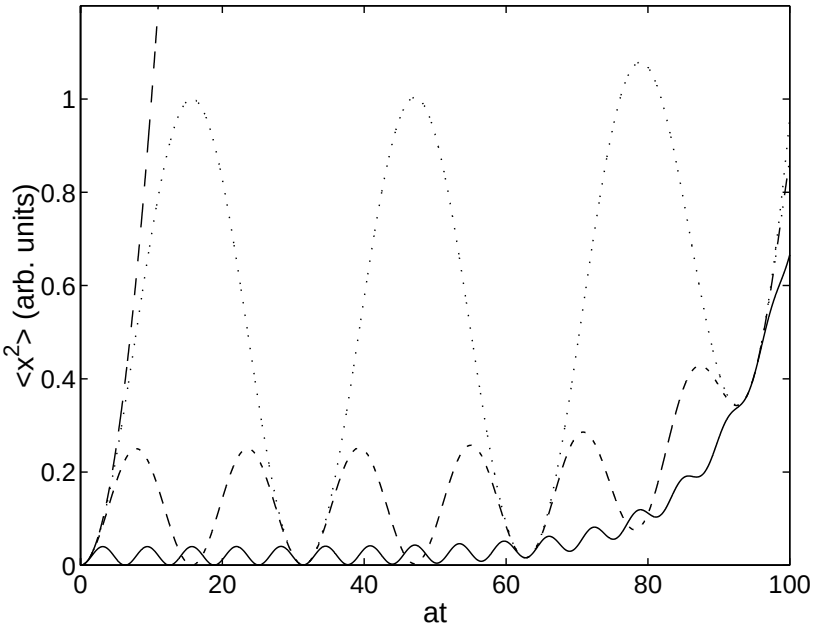

Fig. 6. Evolution of $\langle x^2\rangle$ for $u_0(x) = (\pi/10)\sinh(\pi/20)[1 + (x/\sigma)^{20}]^{-1}$ versus at with $\omega\sigma/v$=0 (dashed line), 0.01 (dotted line), 0.002 (dash-dotted line), and 0.05 (solid line), respectively. Because u broadens as time evolves, $\langle x^2\rangle$ increases in time.

The first term in $\langle x^2\rangle$ in Eq. (16) arises from the oscillation in the medium velocity. The second term represents two simultaneous effects: an increase of the area of the distribution, and a displacement of the distribution from the origin. If $p(y,t)$ and $y^2 p(y,t)$ are integrable over all space, the time dependence of $\langle x^2\rangle$ can be determined analytically.

For an initial condition $u_0(x) = [1 + (|x|/\sigma)^\alpha]^{-1}[\alpha \sinh(\pi/\alpha)]/(2\pi)$, we have the explicit analytical result

$$\langle x^2\rangle = \left(\frac{v}{\omega\sigma}\right)^2 [\sin^2(\omega t)] + \frac{\sinh(\pi/\alpha)}{\sinh(3\pi/\alpha)}\left[1 + \frac{b\alpha\sinh(\pi/\alpha)}{a2\pi}(\mathrm{e}^{at} - 1)\right]^{2/\alpha}. \tag{17}$$

Exponential growth coexists with an oscillation at frequency 2ω. In Fig. 6 we have plotted $\langle x^2\rangle$ for initial power law tails for different values of the ratio $\delta = \omega\sigma/v$. When the medium velocity is constant, the oscillating term in Eq. (17) becomes quadratic in time. Any value of δ different from zero gives rise to oscillations. However, as δ increases, the oscillations gradually disappear since the frequency of the velocity sign reversal is so high that u remains essentially centered around the origin while its area increases. Analytically, we can also see in Eq. (17) that, as the exponential term increases, the relative value of the oscillating term to the exponential term goes to zero.

3.2. Time-dependent growth rate

Eq. (13) shows that, for a constant velocity v but a time-dependent growth rate, we have

$$u(x,t) = \frac{1}{(\mathrm{e}^{-\int_0^t \mathrm{d}s\, a(s)}/u_0(x - vt)) + b\int_0^t \mathrm{d}t'\, \mathrm{e}^{-\int_{t'}^t \mathrm{d}s\, a(s)}}. \tag{18}$$

Given the special form of this solution, it is possible to draw general conclusions about its long-time behavior simply through the analysis of the time-averaged $\widehat{u(t)}$ of the corresponding logistic equation (i.e., Eq. (11) without the velocity term and with b constant). The corresponding solution when the velocity term is included can be thought

of as an evolution of u subject to a logistic nonlinearity whose initial value u_0 is displaced in space to the right. The time-averaged solution of the logistic equation can be written out explicitly as

$$\widehat{u(t)} = \frac{1}{T}\int_0^T u(t)\,\mathrm{d}t = \frac{1}{b}\frac{\ln\left[1/u_0 + b\,\mathrm{e}^{-A(0)}\int_0^T \mathrm{d}t'\,\mathrm{e}^{B(t')}\right]}{T}, \tag{19}$$

where $B(t) = \int_0^t \mathrm{d}s\,a(s)$, and T is an appropriate interval. If

$$\lim_{T\to+\infty}\widehat{u(t)} \simeq \frac{1}{b}\frac{\ln\left[\int_0^T \mathrm{d}t'\,\mathrm{e}^{B(t')}\right]}{T} \to 0 \tag{20}$$

$u(t)$ will decay to zero at long times. On the other hand, if the above limit is different from zero, the logistic equation will have a non-zero solution at long times. If a is constant, $\int_0^T \mathrm{d}t'\exp[B(t')]$ equals $[\exp(aT)-1]/a$ with a/b as the long-time average. If $a(t) = \varepsilon + a\cos(\omega t)$ with $\varepsilon \geq 0$, $\exp[B(t)]$ can be expanded in I-Bessel functions:

$$\lim_{T\to+\infty}\widehat{u(t)} \simeq \frac{\varepsilon}{b} + \frac{1}{T}\ln\left[I_0\left(\frac{a}{\omega}\right) + \sum_{k=1}^{\infty} g_k(\omega T)\right], \tag{21}$$

where $g_k(\omega T)$ is a periodic function of ωT, and $\sum_{k=1}^{\infty} g_k(\omega T)$ is a convergent series. Eq. (21) shows that $\widehat{u(t)}$ cannot tend to a vanishing value for any $\varepsilon > 0$. Therefore, $u(t)$ will not decay. If $\varepsilon = 0$, we have

$$\lim_{T\to+\infty}\widehat{u(t)} \simeq \frac{1}{T}\ln\left\{\left[2\sum_{k=1}^{\infty}(-1)^k I_{2k}\left(\frac{a}{\omega}\right)\frac{\sin(2k\omega T)}{2k\omega T} - 2\sum_{k=0}^{\infty}(-1)^k I_{2k+1}\left(\frac{a}{\omega}\right)\frac{\cos((2k+1)\omega T)}{(2k+1)\omega T}\right]\right\}, \tag{22}$$

which shows a decay to zero as $T \to +\infty$. We have tested these predictions numerically from Eq. (18). At long times, u decays to zero if Eq. (20) is satisfied. For such a case, as u moves to the right, it broadens and its peak value at each cycle of the oscillation of $a(t)$ decreases until u reaches the value zero uniformly. If, instead, Eq. (20) is not satisfied, as u broadens, its peak value at each oscillation is always the same. For $u_0(x)$ with compact support, Eq. (20) can still be applied to predict the long-time behavior, the evolution being different only in that u does not broaden.

3.3. Spatially dependent growth rate

We now return to Eq. (2) and take the growth coefficient to have a spatial dependence $a(x)$, and the velocity v to be constant. The resulting equation for $\phi = 1/u$,

$$\frac{\partial\phi(x,t)}{\partial t} + v\frac{\partial\phi(x,t)}{\partial x} + a(x)\phi(x,t) = b(x,t), \tag{23}$$

can be solved using a method recently employed in the study of carrier velocity saturation in organic materials [18]. The general solution is

$$\phi(x,t) = \mathrm{e}^{-(1/v)\int_{x-vt}^{x}\mathrm{d}x'\,a(x')}\phi_0(x-vt) + \int_0^t \mathrm{d}t'\,\mathrm{e}^{-(1/v)\int_{x-v(t-t')}^{x}\mathrm{d}x'\,a(x')}b(x-v(t-t'),t'), \tag{24}$$

leading, for the case of constant b, to

$$u(x,t) = \frac{1}{(\mathrm{e}^{-(1/v)\int_{x-vt}^{x}\mathrm{d}x'\,a(x')}/u_0[x-vt]) + b\int_0^t \mathrm{d}t'\,\mathrm{e}^{-(1/v)\int_{x-vt'}^{x}\mathrm{d}x'\,a(x')}}. \tag{25}$$

In the context of bacteria in a Petri dish [3], the inhomogeneity in the growth rate could represent a localized distribution of food from which a population is driven away. In order to mimic harsh conditions of survival, $a(x)$ is

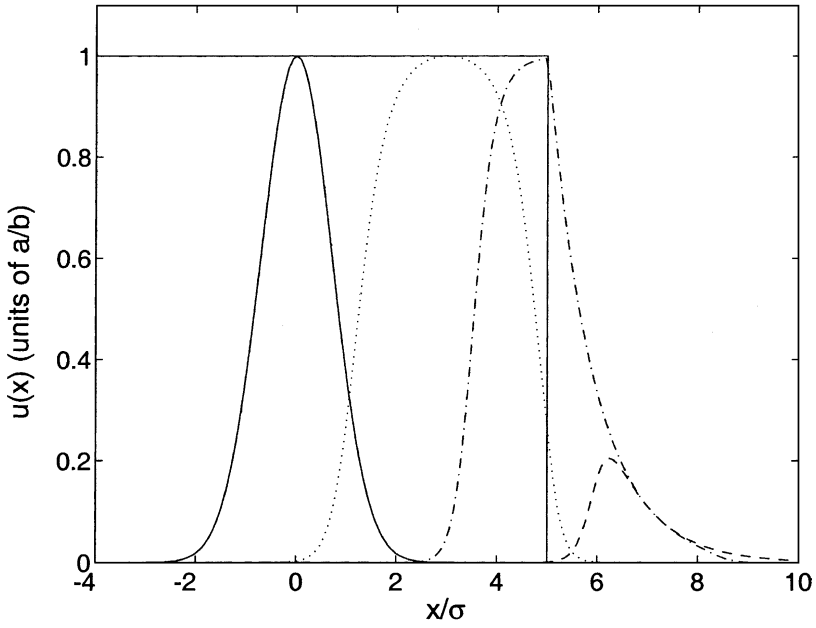

Fig. 7. Evolution with an initial $u_0(x) = \exp(-x^2/\sigma^2)$, and the following inhomogeneous growth coefficient: $a(x) = a\{(0.55)\Theta[(x/\sigma) + 5] - \Theta[(x/\sigma) - 5] - 0.1\}$. The solid line centered around the origin, the dotted line, the dash-dotted line, and the dashed line correspond, respectively, to $t = 0$, 3, 6, 9 in units of $1/a$. As the distribution is pushed out of the region of positive growth, its peak value decreases and eventually decays to zero. For clarity, we have also plotted (solid line) the profile $a(x)/b$ in the region of the mask which occupies the interval $(-5 \leq x/\sigma \leq 5)$ in which $a(x)$ is positive. Parameters are $v/(a\sigma) = 1$, and $\sigma/L = 0.1$ where L is the total width of the mask.

chosen to be negative (or zero) for large $|x|$. We have seen that in Section 2 a population can propagate in a direction opposite to that of the medium velocity. Therefore, it is natural to ask whether a population subjected to Eq. (2) can survive when regions of positive growth are confined to a finite segment.

The evolution is as follows. As for the homogeneous case, the spatial dependence at large x determines the direction and the velocity of propagation of the leading edges. As shown in Section 2, all those initial conditions that have a $\bar{u}(x)$ for $x \to -\infty$ steeper than $\exp(ax/v)$, simply grow to the saturation value and move to the right. Since the saturation value is now x-dependent, u adjusts its value to the profile $a(x)/b$, while drifting to the right. In particular, once the region where $a(x)/b < 0$ is reached, u decays to zero at a rate equal to $|a(x)|$. It should be noted that, even when $a(x) = 0$ rather than being negative, u decays but the decay is slower, i.e., not exponential but algebraic: $(bt)^{-1}$. In Fig. 7 we show an example with $a(x)$ positive inside a region of width L around the origin and negative outside it.

On the other hand, for an initial condition whose $\bar{u}(x)$ for $x \to -\infty$ is shallower than $\exp(ax/v)$, the left leading edge moves to the left until the left boundary of the mask is reached. At that point, an inversion in the velocity direction occurs and the left front starts moving to the right. Eventually, u is pushed outside the region of positive growth and decays to zero as in Fig. 7. The inversion in the velocity of the left front is due to the fact that $\bar{u}(x)$ is changing its dependence from shallow to steep. In the region where $a(x)$ is negative, the growth coefficient is actually a coefficient of linear loss, which, together with the saturation coefficient, contributes to make the spatial profile steeper. Once the left profile has become steeper than $\exp(ax/v)$, the left leading edge reverses its velocity direction. From then on, the evolution is as for a steep initial condition described above. If the left leading edge has a profile exactly equal to $\exp(ax/v)$ for $x \to -\infty$, the left face settles initially into the front solution with velocity $c = 0$, but, once the profile for large x becomes steeper than $\exp(ax/v)$, the growth coefficient cannot balance perfectly

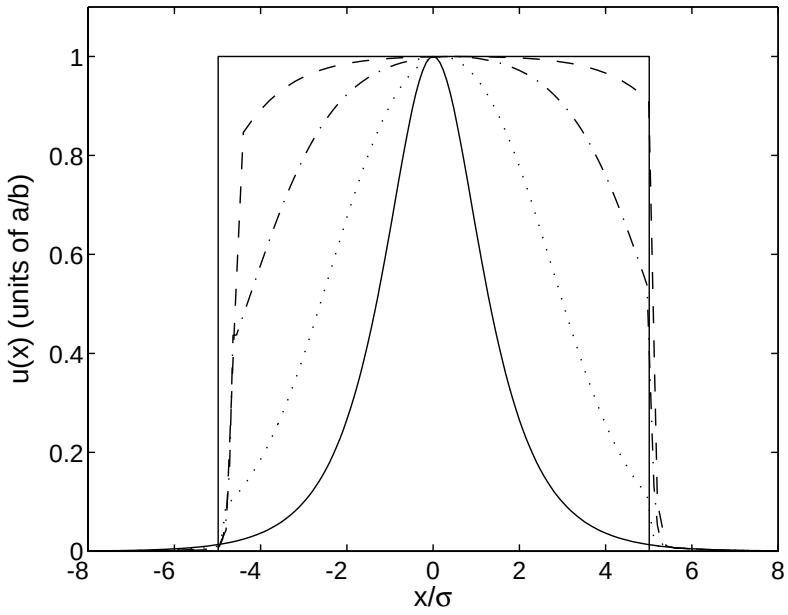

Fig. 8. Evolution for an initial $u_0(x) = \mathrm{sech}(x/\sigma)$ with the inhomogeneous growth coefficient as in Fig. 7. The solid line, the dotted line, the dash-dotted line, and the dashed line correspond, respectively, to $t = 0$, 2, 4, 6 in units of $1/a$. Parameters are $v/(a\sigma) = 0.1$, and $\sigma/L = 0.1$ where L is the total width of the mask.

the movement to the right, the velocity c becomes positive, u is pushed outside the region of positive growth and decays to zero. In Fig. 8 we have plotted an example for a shallow initial condition with an $a(x)$ as in Fig. 7.

4. Stability analysis

Stability analysis is obviously of great importance to the solutions of an equation such as (2). We perform such an analysis for the case of constant coefficients discussed in Section 2. There are three steady-state solutions of Eq. (3): two are homogeneous in space ($u = 0$ and $u = a/b$), and the third is inhomogeneous. Of these, $u = 0$ is clearly unstable due to the presence of the growth coefficient a. For $u = a/b$, we rewrite Eq. (3) as $u(x, t) = a/b + f(x, t)$ where f represents a generic finite perturbation, and obtain

$$\frac{\partial f(x,t)}{\partial t} + v\frac{\partial f(x,t)}{\partial x} = -af(x,t) - bf^2(x,t). \tag{26}$$

For any finite f, Eq. (26) shows a decay due to both a linear and a nonlinear term and a movement to the right with velocity v, thus demonstrating the stability of the steady state $u = a/b$. Solving Eq. (3) without time dependence allows us to write the inhomogeneous steady state

$$u_{\mathrm{s.s.}}(x) = \frac{a}{b}\frac{1}{1 + \mathrm{e}^{-(a/v)x}}, \tag{27}$$

which implies that, to the left of the origin, $u(x)$ is exponentially equal to zero while, to the right of the origin, it is exponentially equal to a/b. Comparison of Eq. (27) with the (left) front profile in Eq. (3), shows that the former is a special case of the latter, the propagation velocity c being equal to zero. The stability of the inhomogeneous steady state can thus be determined from the stability of the front solution.

For the front solution we write Eq. (3) in the moving frame of reference, i.e. with $u(x,t) = U(z,t)$ where $z = x - ct$, we have

$$\frac{\partial U(z,t)}{\partial t} + (v-c)\frac{\partial U(z,t)}{\partial z} = aU(z,t) - bU(z,t)^2. \tag{28}$$

Substituting $U(z,t) = u_{\text{front}}(z) + f(z,t)$ into Eq. (28) we get, for the perturbation $f(z,t)$ from the front,

$$\frac{\partial f(z,t)}{\partial t} + (v-c)\frac{\partial f(z,t)}{\partial z} = (a - 2bu_{\text{front}}(z))\, f(z,t) - bf^2(z,t). \tag{29}$$

We consider also the nonlinear term f^2 in Eq. (29). The reason is that a simple linearization does not allow us to determine the stability of the front, since the corresponding eigenvalue is exactly equal to zero. Using Eq. (25), Eq. (29) can be solved exactly to yield

$$f(z,t) = \frac{(1+\mathrm{e}^{-at}\,\mathrm{e}^{(a/(v-c))z})^2(1+\mathrm{e}^{(a/(v-c)z)})}{(\mathrm{e}^{-at}(1+\mathrm{e}^{(a/(v-c))z})^3/f_0[z-(v-c)t]) + (b/a)(1-\mathrm{e}^{-at})(1+\mathrm{e}^{-at}\,\mathrm{e}^{(a/(v-c))z})}, \tag{30}$$

where $f_0(z)$ is the perturbation in the moving frame at time $t = 0$. Plotting the evolution of Eq. (30) for various initial conditions, we have found the following. For any f_0 which is either finite or has tails steeper than an exponential, Eq. (30) shows a decay to zero together with a movement to the right. On the contrary, for perturbations which have exponential tails or have tails shallower than exponential, Eq. (30) shows unbounded growth. When the front is a step profile, i.e., when $c = v$, the stability analysis in the moving frame turns out easier if we separate the analysis into two regions: one where $u = a/b$ (region I) and one where $u = 0$ (region II). Then,

$$f_{\text{I}}(z,t) = \frac{f_{\text{I}}(z,0)}{\mathrm{e}^{at} + (b/a)(1+\mathrm{e}^{at})\, f_{\text{I}}(z,0)}, \tag{31}$$

$$f_{\text{II}}(z,t) = \frac{f_{\text{II}}(z,0)}{\mathrm{e}^{-at} + (b/a)(1-\mathrm{e}^{-at})\, f_{\text{II}}(z,0)}. \tag{32}$$

Any finite f_{I} decays to zero exponentially. Any finite f_{II} shows an exponential growth to the value a/b. Since Eq. (32) shows that the full spatial extent of the perturbing f_{II} grows to the value a/b, it means that the front is translated by an amount equal to the extent of $f_{\text{II}}(z,0)$. For a right front, the shift is in the direction of the medium velocity while for a left front it is opposite to the medium velocity. This analysis is compatible with the dynamics studied in Section 2 for initial conditions with compact support. We have observed there that, independently of the form of $u_0(x)$, the system evolves into a step profile with height a/b and width given by the width of the support. In other words, any finite perturbation to a step profile does not change its velocity or its shape. It simply translates the step profile by a finite amount.

We thus see that a given leading edge for any initial condition is attracted either to the homogeneous steady state $u = a/b$ or to a front solution. If a leading edge has compact support, it settles into the front solution with velocity $c = v$. If the left (right) leading edge of u_0 goes to zero as $\exp(x/\sigma)(\exp(-x/\sigma))$ for $x \to -\infty$ ($x \to +\infty$), it settles into the front solution with velocity $c = v - a\sigma$ ($c = v + a\sigma$). If the left (right) leading edge has a decay to zero for $x \to -\infty$ ($x \to +\infty$), qualitatively steeper than an exponential, it is attracted to the step profile front solution. On the other hand, if the initial left (right) leading edge has a decay to zero for $x \to -\infty$ ($x \to +\infty$) qualitatively shallower than an exponential, it is attracted to the steady-state solution $u = a/b$. In other words, if the initial distribution has non-exponential tails, it cannot settle to any front solution: the spatial dependence of the tails cannot match any exponential shape. In terms of phase space trajectories we can say the following: a left (right) leading edge steeper than an exponential is in the basin of attraction of the left (right) front solution with velocity $c = v$, while a left (right) leading edge shallower than an exponential is in the basin of attraction of the steady state. If an initial condition has its left (right) profile exponentially decaying for $x \to -\infty$ ($+\infty$), it represents a small

perturbation to the stable front solution with a specific velocity c. As time grows, the finite perturbation decays to zero and the left (right) edge of u becomes exactly as in Eq. (6). This analysis can help us understand Fig. 4. The superlinear increase in Fig. 4 can be understood occurring because u is increasing its velocity and decreasing its steepness in order to reach the attracting steady state $u = a/b$. Similarly, the sublinear increase occurs because u is decreasing its velocity and increasing its steepness in order to reach the attracting step profile front solution.

The spatial dependence of the left leading edge of $u_0(x)$ determines whether there is a bifurcation in the behavior at long times. If $\bar{u}(x)$ is shallower than $\exp(ax/v)$ for $x \to -\infty$, the left leading edge moves to the left and u becomes equal to a/b in the left semi-infinite space. If, on the contrary, $\bar{u}(x)$ is steeper than $\exp(ax/v)$ for $x \to -\infty$, it moves to the right and u represents a traveling wave solution to the right. The right leading edge does not play any role in the bifurcation because, independently of its shape, is always traveling to the right, making $u = a/b$ in the semi-infinite right space at long times. Finally, if $u_0(x) \sim \exp(ax/v)$ for $x \to -\infty$, the long-time behavior is the inhomogeneous steady state given in Eq. (27).

5. Conclusions

In this paper, we have analyzed the effect of convection on the evolution of a population which follows logistic growth. Interesting phenomena emerge. For the case of constant coefficients, the propagation direction of the left leading edge (the right leading edge if v is to the left) can, under certain conditions, be *opposite* to the direction of the medium velocity. This effect is responsible for a bifurcation in the long-time behavior of the solutions. If the initial population has a left tail shallower than $\exp(ax/v)$, the steady state is the spatially homogenous solution $u = a/b$. If the left tail is steeper than $\exp(ax/v)$, the solution is a traveling wave solution. If the left tail is exactly equal to $\exp(ax/v)$, the steady state is spatially inhomogeneous. We have also observed a curious phenomenon of velocity inversion, wherein the left face can first move in one direction and then reverse direction, and have studied the case of coefficients which depend on time and space. This analysis has been made possible by the considerably greater simplicity of the nonlinear convective equation (2) relative to equations such as the Fisher equation which is diffusive rather than convective.

It is important to ask whether the results we have obtained analytically from Eq. (2) are changed substantially, or only slightly, when a small diffusion constant D is introduced. To answer that question, we have carried out *numerical* analysis of Eq. (1) for several initial profiles considered analytically above from Eq. (2). We chose the dimensionless parameter Da/v^2 as an indicator of the amount of diffusion introduced. When the values of that parameter (the square of the ratio of half the Fisher velocity to the convection velocity) were small, the departure from our analytic results were found to be small. The departure was found to occur more quickly when Da/v^2 was increased. In addition, diffusion tended to smooth out the profiles. Preliminary studies along these lines suggest that richer evolution could result from an interplay of drift and diffusion in specialized cases. We will report on these possibilities elsewhere.

Our exact solutions of the simplified equation (2) are useful in two ways. The first is for direct application to systems such as bacterial colonies in a Petri dish in which, either as a result of genetic engineering or the preparation of the environment, the diffusion is negligible (by contrast, the convection is produced mechanically and controllably by moving a mask, see [3,4]). The second is in using our solutions of (2) as an aid in addressing the more complex Fisher equation. Our ongoing work concerning the latter issue also includes comparison of the exact solutions presented in this paper to analytic solutions of several other different but related equations: the Montroll [14] and the Rotenberg [15] equations which add further nonlinear terms to the Fisher equation to ensure analytic solutions, the *bidirectional* wave equation with logistic nonlinearity whose traveling wave solutions have been obtained analytically by Abramson et al. [10], and the Fisher equation in the steady state analyzed in the bacterial context [16,19] as well as in ecological contexts such as in the study of phytoplankton distributions [20].

Acknowledgements

We thank Dr. Marcelo Kuperman for useful conversations and acknowledge the partial support of this work by the Los Alamos National Laboratory via a grant made to the University of New Mexico (Consortium of The Americas for Interdisciplinary Science) and by the National Science Foundation's Division of Materials Research via grant No. DMR0097204.

References

[1] E. Ben-Jacob, I. Cohen, H. Levine, Cooperative self-organization of microorganisms, Adv. Phys. 49 (2000) 395–554.
[2] J. Wakita, K. Komatsu, A. Nakahara, T. Matsuyama, M. Matsushita, Experimental investigation on the validity of population dynamics approach to bacterial colony formation, J. Phys. Soc. Jpn. 63 (1994) 1205–1211.
[3] A.L. Lin, B. Mann, G. Torres, B. Lincoln, J. Kas, H.L. Swinney, Localization and extinction of bacterial populations under inhomogeneous growth conditions, Preprint.
[4] B. Mann, Spatial phase transitions in bacterial growth, Ph.D. Thesis, 2001, Unpublished.
[5] D.R. Nelson, N.M. Shnerb, Non-Hermitian localization and population biology, Phys. Rev. E 58 (1998) 1383–1403; K.A. Dahmen, D.R. Nelson, N.M. Shnerb, Life and death near a windy oasis, J. Math. Biol. 41 (2000) 1–23.
[6] R.A. Fisher, The wave of advance of advantageous genes, Ann. Eugenics 7 (1937) 355–369.
[7] J.D. Murray, Mathematical Biology, 2nd ed., Springer, New York, 1993.
[8] K.K. Manne, A.J. Hurd, V.M. Kenkre, Nonlinear waves in reaction–diffusion systems: The effect of transport memory, Phys. Rev. E 61 (2000) 4177–4184.
[9] G. Abramson, A.R. Bishop, V.M. Kenkre, Effects of transport memory and nonlinear damping in a generalized Fisher's equation, Phys. Rev. E 64 (2001) 066615/1–066615/6.
[10] G. Abramson, V.M. Kenkre, A.R. Bishop, Analytic solutions for nonlinear waves in coupled reacting systems, Physica A 305 (2002) 427–436.
[11] G. Abramson, V.M. Kenkre, Spatiotemporal patterns in the Hantavirus infection, Phys. Rev. E 66 (2002) 011912/1–011912/5.
[12] M.A. Aguirre, G. Abramson, A.R. Bishop, V.M. Kenkre, Simulations in the mathematical modeling of the spread of the Hantavirus, Phys. Rev. E 66 (2002) 041908-13.
[13] J.N. Mills, T.L. Yates, T.G. Ksiazek, C.J. Peters, J.E. Childs, Long-term studies of hantavirus reservoir populations in the southwestern United States: rationale, potential, and methods, Emerg. Infect. Dis. 5 (1999) 95–101.
[14] E.W. Montroll, On nonlinear processes involving population growth and diffusion, J. Appl. Probab. 4 (1967) 281–290.
[15] M. Rotenberg, Diffusive logistic growth in deterministic and stochastic environments, J. Theor. Biol. 94 (1982) 253–280.
[16] V.M. Kenkre, M.N. Kuperman, Applicability of the Fisher equation to bacterial population dynamics, scheduled for publication, Phys. Rev. E. 67 (2003) 051921-5.
[17] D. Mollison, Spatial contact models for ecological and epidemic spread, J. Roy. Stat. Soc. B 39 (1977) 283–326.
[18] V.M. Kenkre, P. Parris, Saturation of charge carrier velocity with increasing electric fields: Theoretical investigations for pure organic crystals, Phys. Rev. B 65 (2002) 205104/1–205104/11.
[19] V. M. Kenkre, Memory functions, nonlinear techniques, and kinetic equation approaches, in: V.M. Kenkre, K. Lindenberg (Eds.), Proceedings of the PASI on Modern Challenges in Statistical Mechanics: Patterns, Noise, and the Interplay of Nonlinearity and Complexity, AIP, 2003, pp. 63–102.
[20] M. Kot, Elements of Mathematical Ecology, Cambridge University Press, Cambridge, 2001.